ISSN 1070-3284, Russian Journal of Coordination Chemistry, 2017, Vol. 43, No. 8, pp. 540–546. © Pleiades Publishing, Ltd., 2017.

Microwave-Assisted Synthesis, Crystal Structures, and in vitro Antibacterial Studies of Zinc(II) and Nickel(II) Complexes with Schiff Bases[1]

W. G. Zhang[a], * and J. H. Liang[b]

[a] *College of Chemistry and Chemical Engineering, Qiqihar University, Qiqihar, 161006 P.R. China*
[b] *Library, Qiqihar University, Qiqihar, 161006 P.R. China*
**e-mail: zhangweiguang1230@163.com*

Received July 21, 2016

Abstract—The syntheses of a mononuclear zinc(II) complex $[ZnCl(L^1)(Amp)]$ (**I**) and a mononuclear nickel(II) complex $[Ni(L^2)(HL^2)](BF_4) \cdot 0.5H_2O$ (**II**) (HL^1 = 4-methyl-2-[(4-methylpyridin-2-ylimino)methyl]phenol, HL^2 = 4-methyl-2-[(pyridin-2-ylmethylimino)methyl]phenol; Amp = 2-amino-4-methylpyridine) were prepared under microwave irradiation. The complexes were characterized by a combination of elemental analyses, and IR and electronic spectra. Their structures were further confirmed by single crystal X-ray crystallography (CIF files CCDC nos 1437737 (**I**), 1437738 (**II**)). The Zn atom in the monomeric complex **I** is in tetrahedral coordination. The Ni atoms in the dimeric complex **II** are in octahedral coordination. Crystals of the complexes are stabilized by hydrogen bonds. In order to evaluate the biological activity of the complexes, in vitro antibacterial against *Staphylococcus aureus*, *Bacillus subtilis*, *Escherichia coli*, and *Pseudomonas aeruginosa* was assayed. The complexes have strong activity against *Bacillus subtilis*.

Keywords: zinc complex, nickel complex, microwave-assisted synthesis, crystal structure, antibacterial activity

DOI: 10.1134/S1070328417080085

INTRODUCTION

In the past few years, microwave-assisted preparation has attracted enormous interest in the fields of coordination chemistry and inorganic synthesis [1–3]. Microwave irradiation can accelerate many chemical reactions. This method of synthesis has also advantages in providing a clean, cheap and easy handling heating way, which achieves not only higher yields with less reaction time, but more complete products [4, 5]. Metal-organic coordination compounds have received great interest in the fields of crystal engineering and functional materials, due to their intriguing structural features as well as mysterious properties. Schiff bases have been known for a long time. Most Schiff bases derived from salicylaldehyde and its analogues are reported to have interesting biological properties [6–8]. When bioorganic molecules or drugs are bound to metal ions, there is drastic change in their biomimetic properties, therapeutic effects and pharmacological properties. Essential metal ions such as manganese and iron and their complexes are found to be antitumor active, catalytic active, antimicrobial and cytotoxic [9–12]. In this study, the synthesis, characterization and antibacterial properties of a mononuclear manganese(III) complex $[Mn(L)(Dca)(OH_2)]$ and a mononuclear zinc(II) complex $[ZnCl(L^1)(Amp)]$ (**I**) and a mononuclear nickel(II) complex $[Ni(L^2)(HL^2)](BF_4) \cdot 0.5H_2O$ (**II**) (HL^1 = 4-methyl-2-[(4-methylpyridin-2-ylimino)methyl]phenol, HL^2 = 4-methyl-2-[(pyridin-2-ylmethylimino)methyl]phenol; Amp = 2-amino-4-methylpyridine), are described.

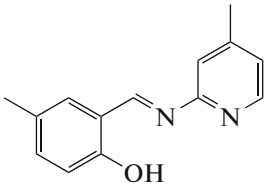

HL^1

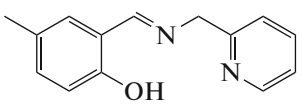

HL^2

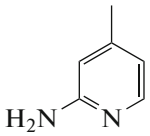

Amp

[1] The article is published in the original.

EXPERIMENTAL

Chemicals and physical measurements. All the starting materials and solvents used in the present investigation were of analytical grade and used without further purification. HL^1 and HL^2 were prepared according to the literature method [13]. WX-4000 microwave digestion system was used in microwave synthesis. Elemental analyses were performed on a Perkin-Elmer 2400 Elemental Analyzer. IR spectra were recorded as KBr pellets on a Bio-Rad FTS 135 spectrophotometer in the range of 4000–400 cm^{-1}. Electronic spectra were recorded on a Lambda 10 spectrometer. Conductivities of 10^{-3} M solutions in acetonitrile were measured on a DDS-11A conductivity meter.

Synthesis of complex I. 5-Methylsalicylaldehyde (27.2 mg, 0.2 mmol), 2-amino-4-methylpyridine (43.2 mg, 0.4 mmol), zinc chloride (27.5 mg, 0.2 mmol), and 20 mL methanol were placed in a 30-mL Teflon-lined autoclave, which was then inserted into the cavity of a microwave reactor. The reaction mixture was maintained at 350 K and 200 W for 10 min. Then natural cooling was followed for about 1 h. The resulting solution was then filtered and allowed to evaporate slowly at room temperature. Colorless block-like single crystals appeared in several days. The crystals were filtered off, washed with water and dried in air. The yield was 53% (based on Zn).

For $C_{20}H_{21}N_4OClZn$

anal. calcd., %:	C, 55.3;	H, 4.9;	N, 12.9.
Found, %:	C, 55.1;	H, 5.0;	N, 13.0.

IR spectrum (ν, cm^{-1}): 3163 w ν(NH), 1609 s ν(C=N). Molar conductance value: 23 Ω^{-1} cm^2 mol^{-1}.

Synthesis of complex II. 5-Methylsalicylaldehyde (27.2 mg, 0.2 mmol), 2-aminomethylpyridine (21.6 mg, 0.2 mmol), ammonium fluoborate (52.0 mg, 0.5 mmol), nickel nitrate hexahydrate (58.2 mg, 0.2 mmol), and 20 mL methanol were placed in a 30-mL Teflon-lined autoclave, which was then inserted into the cavity of a microwave reactor. The reaction mixture was maintained at 350 K and 200 W for 10 min. Then natural cooling was followed for about 1 h. The resulting solution was then filtered and allowed to evaporate slowly at room temperature. Green block-like single crystals appeared in several days. The crystals were filtered off, washed with water and dried in air. The yield was 41% (based on Ni).

For $C_{56}H_{56}B_2N_{85}OF_8Ni_2$

anal. calcd., %:	C, 55.5;	H, 4.7;	N, 9.2.
Found, %:	C, 55.7;	H, 4.6;	N, 9.4.

IR spectrum (ν, cm^{-1}): 3440 m ν(O–H), 1621 s ν(C=N), 1080 s ν(BF_4). Molar conductance value: 118 Ω^{-1} cm^2 mol^{-1}.

X-ray structure determination. Single-crystals X-ray diffraction analyses of the complexes were carried out on a Bruker Smart Apex CCD diffractometer equipped with a graphite monochromated MoK_α radiation (λ = 0.71073 Å) at 298(2) K. Raw frame data were integrated with the SAINT program [14]. The structures were solved by direct methods with SHELXS-97 and refined by full-matrix least-squares on F^2 using SHELXS-97 [15]. An empirical absorption correction was applied with the program SADABS [16]. All non-hydrogen atoms were refined anisotropically. The hydrogen atoms of the hydroxyl groups in complex **II** were located from an electronic density map. Molecular graphics software used was ORTEP III [17]. The crystal data for the complexes are listed in Table 1. Selected bond lengths and angles for the complexes are listed in Table 2.

Supplementary material for structures has been deposited with the Cambridge Crystallographic Data Centre (CCDC nos. 1437737 (**I**) and 1437738 (**II**); deposit@ccdc.cam.ac.uk or http://www.ccdc.cam.ac.uk).

In vitro antibacterial assay. The Schiff base ligands and the complexes were screened in vitro for their antibacterial property against two Gram-positive (*Staphylococcus aureus* MTCC 96, *Bacillus subtilis* MTCC 121) and two Gram-negative (*Escherichia coli* MTCC 1652, *Pseudomonas aeruginosa* MTCC 741) bacterial strains by agar well diffusion method [18]. DMSO was used as a negative control, and Ciprofloxacin was used as positive control.

Determination of minimum inhibitory concentration (MIC). MIC of the compounds against bacterial strains was tested through a modified agar well diffusion method [19]. A twofold serial dilution of each compound was prepared by first reconstituting the compound in DMSO followed by dilution in sterile distilled water to achieve a decreasing concentration range 256 μM. A 100 μL volume of each dilution was introduced into wells in the agar plates already seeded with 100 μL of standardized inoculums (10^6 cfu mL^{-1}) of the test microbial strain. All test plates were incubated aerobically at 37°C for 24 h and observed for the inhibition zones.

RESULTS AND DISCUSSION

The IR spectra of the Schiff base ligands and the complexes provide information about the metal-ligand bonding. The infrared spectra of the complexes are fully consistent with their crystal structures. The weak band at 3163 cm^{-1} is attributable to ν(N–H) stretching of complex **I**. The broad band centered at 3440 is attributable to ν(O–H) stretching of complex **II**. The infrared spectrum of complex **II** displays

Table 1. Crystallographic data collection and structure refinement of structures **I** and **II**

Parameter	Value	
	I	**II**
Formula weight	434.2	1212.1
Crystal system	Triclinic	Monoclinic
Space group	$P\bar{1}$	$P2_1/c$
a, Å	7.9046(7)	14.1401(12)
b, Å	11.2567(10)	22.2989(19)
c, Å	12.9284(13)	17.8987(14)
α, deg	114.677(9)	90.00
β, deg	97.627(8)	97.733(2)
γ, deg	99.973(8)	90.00
V, Å^3	1002.13(16)	5592.3(8)
Z	2	4
ρ_{calcd}, g cm^{-3}	1.439	1.440
μ, mm^{-1}	1.375	0.756
F(000)	448	2504
Reflections collected	7364	48144
Unique reflections	3550	9989
R_{int}	0.0539	0.0893
Observed reflections ($I > 2\sigma(I)$)	2795	5594
Restraints/parameters	0/247	60/740
Final R indices ($I > 2\sigma(I)$)*	0.0901	0.0812
R indices (all data)*	0.2161	0.1779
Goodness-of-fit on F^2	1.080	1.059
$\Delta\rho_{max}$, $\Delta\rho_{min}$, e Å^{-3}	1.693, −0.443	0.953, −0.462

* $R = \Sigma(|F_o - F_c|)/\Sigma|F_o|$, $wR = \{\Sigma[w(|F_o - F_c|)^2]/\Sigma[w|F_o|^2]\}^{1/2}$.

an intense band at 1080 cm^{-1}, which can be assigned to the vibrations of the BF_4 anions. Strong absorptions at about 1640 cm^{-1} in the spectra of HL^1 and HL^2 are assigned to the azomethine groups, ν(C=N). These bands undergo negative shift in the complexes, 1609 cm^{-1} for **I** and 1621 cm^{-1} for **II**, which can be attributed to donation of the nitrogen atom lone pair of the azomethine groups to the metal ions [20]. This assignment is further supported by the presence of medium bands in the 400–650 cm^{-1} region for the complexes, which can be assigned to ν(M–N) and ν(M–O).

Single crystal X-ray diffraction analysis of complex **I** revealed that it is a monomeric mononuclear zinc complex. The labeled diagram of the complex is presented in Fig. 1a.

The Zn ion of the complex is coordinated by one Schiff base ligand, one 2-amino-4-methylpyridine ligand, and one Cl anion. The Schiff base ligand coordinates to the Zn ion by the phenolate oxygen (O(1)) and the imino nitrogen (N(1)). The 2-amino-4-methylpyridine ligand coordinates to the Zn ion through the pyridine nitrogen (N(3)). As a result, the Zn ion adopts a tetrahedral coordination. All the bond lengths and bond angles found for this complex are comparable to those in similar zinc(II) complexes with tetrahedral coordination [21, 22]. The six-membered chelate rings have Zn ion slightly displaced from the mean plane of the ligand atoms. Deviation of Zn(1) atom from the mean plane N(1)–C(8)–C(1)–C(2)–O(1) is 0.127(3) Å. There forms an intramolecular N(4)–H(4*A*)···O(1) hydrogen bond (Table 3), which made the dihedral angle between the Schiff base ligand and the 2-amino-4-methylpyridine ligand of 74.3(5)°. In the molecular packing structure of the complex, molecules are linked through intermolecular N(4)–H(4*B*)···Cl(1) hydrogen bonds (Table 3), to form chains down the x axis (Fig. 2a).

Single crystal X-ray diffraction analysis of complex **II** revealed that it is a hydrogen bonds linked dimeric nickel complex. The labeled diagram of the complex is presented in Fig. 1b.

Table 2. Selected bond lengths (Å) and bond angles (deg)

Bond	*d*, Å	Bond	*d*, Å
		I	
Zn(1)–O(1)	1.970(5)	Zn(1)–N(1)	2.017(6)
Zn(1)–N(3)	2.041(6)	Zn(1)–Cl(1)	2.225(2)
		II	
Ni(1)–O(1)	2.049(4)	Ni(1)–O(2)	2.075(4)
Ni(1)–N(1)	2.018(5)	Ni(1)–N(2)	2.104(5)
Ni(1)–N(3)	2.003(5)	Ni(1)–N(4)	2.086(5)
Ni(2)–O(3)	2.066(4)	Ni(2)–O(4)	2.086(4)
Ni(2)–N(5)	2.013(6)	Ni(2)–N(6)	2.095(6)
Ni(2)–N(7)	1.994(6)	Ni(2)–N(8)	2.087(5)
Angle	ω, deg	Angle	ω, deg
		I	
O(1)Zn(1)N(1)	91.6(2)	O(1)Zn(1)N(3)	105.9(2)
N(1)Zn(1)N(3)	115.0(2)	O(1)Zn(1)Cl(1)	107.9(2)
N(1)Zn(1)Cl(1)	124.4(2)	N(3)Zn(1)Cl(1)	108.8(2)
		II	
N(3)Ni(1)N(1)	175.0(2)	N(3)Ni(1)O(1)	96.51(18)
N(1)Ni(1)O(1)	88.5(2)	N(3)Ni(1)O(2)	88.63(18)
N(1)Ni(1)O(2)	91.60(18)	O(1)Ni(1)O(2)	87.35(16)
N(3)Ni(1)N(4)	80.4(2)	N(1)Ni(1)N(4)	99.7(2)
O(1)Ni(1)N(4)	89.50(18)	O(2)Ni(1)N(4)	168.21(18)
N(3)Ni(1)N(2)	95.0(2)	N(1)Ni(1)N(2)	80.0(2)
O(1)Ni(1)N(2)	168.45(19)	O(2)Ni(1)N(2)	92.44(18)
N(4)Ni(1)N(2)	92.9(2)	N(7)Ni(2)N(5)	177.1(2)
N(7)Ni(2)O(3)	93.5(2)	N(5)Ni(2)O(3)	88.28(19)
N(7)Ni(2)O(4)	87.1(2)	N(5)Ni(2)O(4)	95.35(19)
O(3)Ni(2)O(4)	85.59(16)	N(7)Ni(2)N(8)	81.1(2)
N(5)Ni(2)N(8)	96.5(2)	O(3)Ni(2)N(8)	94.22(18)
O(4)Ni(2)N(8)	168.2(2)	N(7)Ni(2)N(6)	98.1(2)
N(5)Ni(2)N(6)	80.4(2)	O(3)Ni(2)N(6)	166.8(2)
O(4)Ni(2)N(6)	88.68(19)	N(8)Ni(2)N(6)	93.8(2)

The asymmetric unit of complex **II** contains two hydrogen bonds linked nickel complex cation, two fluoborate anions and one water molecule. Each Ni ion of the complex is coordinated by two Schiff base ligands. One is deprotonated, and the other one is neutral. The hydroxyl H atom of the neutral Schiff base ligand linked to the phenolate oxygen of the deprotonated Schiff base ligand of another mononuclear nickel complex. Both the deprotonated and the neutral Schiff base ligands coordinate to the Ni ion through the phenolate of phenol oxygen, imino nitrogen and pyridine nitrogen. The Ni ions are in octahedral coordination. As expected, the Ni–O_{phenol} bonds (2.075(4) and 2.086(5) Å) are a little longer than the Ni–$O_{phenolate}$ bonds (2.049(4) and 2.066(4) Å). All the bond lengths and bond angles found for this complex are comparable to those in similar nickel(II) complexes with octahedral coordination [23, 24]. Crystal

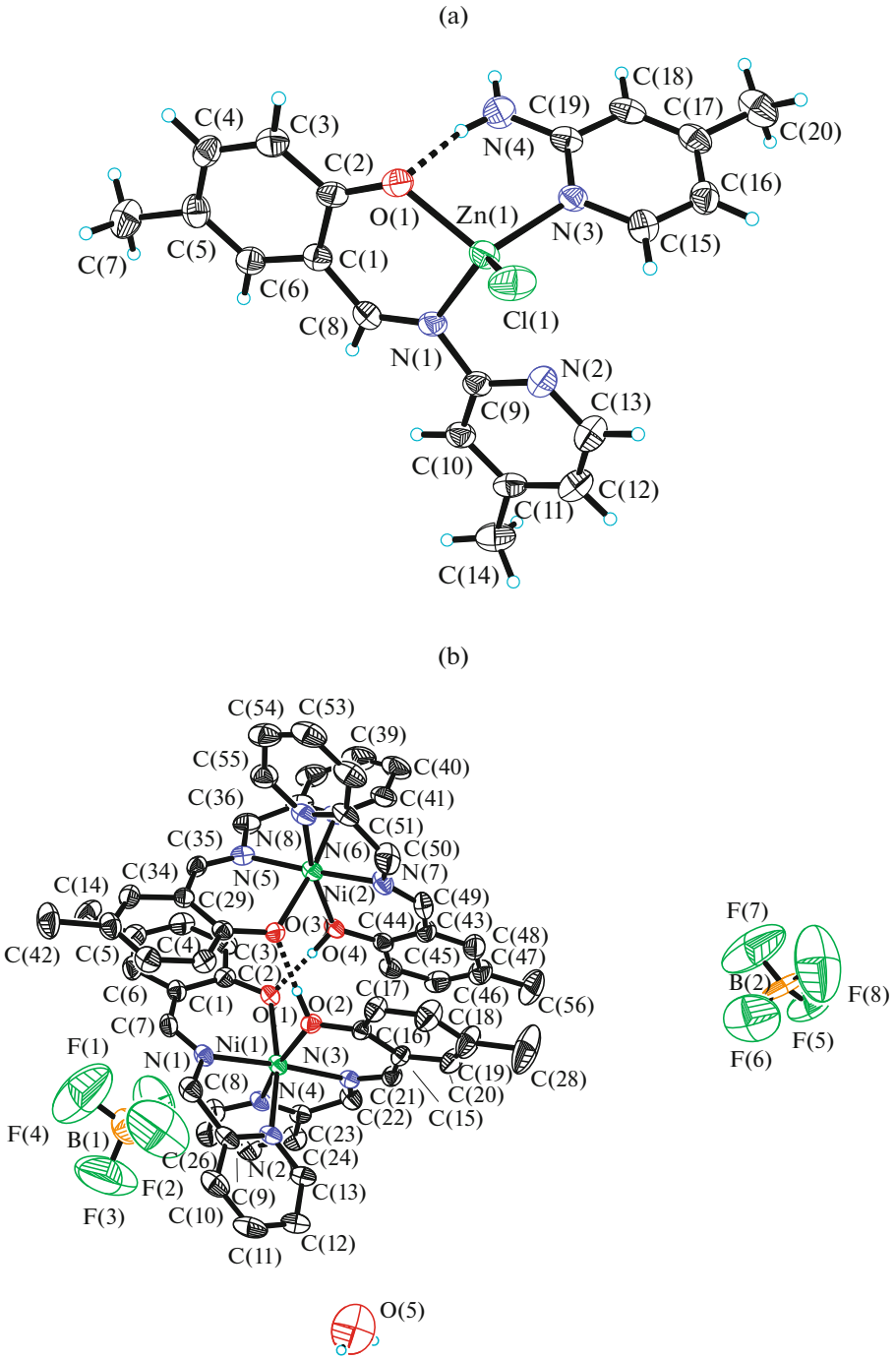

Fig. 1. ORTEP diagram of complexes **I** (a) and **II** (b) with atom labeling scheme. Thermal ellipsoids are at 30% probability level. Hydrogen bond are shown as a dotted line.

structure of the complex is stablize by hydrogen bonds (Table 3, Fig. 2b).

The antibacterial results are listed in Tables 4 and 5. The studies suggested that the two complexes showed somewhat enhanced antibacterial activities in comparison to the free Schiff bases HL^1 and HL^2. Ciprofloxacin produced significantly sized inhibition zones against the tested bacteria, while DMSO, the negative control, produced no inhibitory effect against any of the tested organisms. The free Schiff bases HL^1 and HL^2 show zone of inhibition ranging 3.0–12.7 mm against the four bacteria. Both complexes have been observed to show increased zone of inhibition against the four bacterial strains as compared to the free Schiff bases. The MIC results suggested that both complexes showed medium activities against the bacterial strains

Table 3. Geometric parameters of hydrogen bonds of complexes **I** and **II**

D–H···A	Distance, Å			Angle D–H···A, deg
	D–H	H···A	D···A	
		I		
N(4)–H(4*B*)···Cl(1)^{i}	0.86	2.55	3.326(8)	150
N(4)–H(4*A*)···O(1)	0.86	2.08	2.884(10)	156
		II		
O(2)–H(2)···O(3)	0.90(1)	1.56(1)	2.466(5)	176(8)
O(4)–H(4)···O(1)	0.90(1)	1.58(2)	2.474(5)	172(7)
O(5)–H(5*A*)···F(6)^{ii}	0.85	2.48	3.00(2)	120

* Symmetry transformations used to generate equivalent atoms: ^{i} $-1+x, y, z$; ^{ii} $1-x; -1-y; 1-z$.

Table 4. Diameter of growth of inhibition zone, mm

Compounds	*Staphylococcus aureus*	*Bacillus subtilis*	*Escherichia coli*	*Pseudomonas aeruginosa*
HL^1	5.3	12.7	6.1	2.5
HL^2	4.5	10.6	3.8	3.0
I	8.2	19.3	7.7	10.5
II	9.4	16.1	6.3	8.2
Ciprofloxacin	25.1	20.8	24.9	22.6

Staphylococcus aureus, *Escherichia coli*, and *Pseudomonas aeruginosa*, and strong activity against *Bacillus subtilis*. MIC results also revealed that the complexes are more effective against the antibacterial strains as compared to the Schiff bases. The results of this study are in accordance with those reported previously [25]. The overtone's concept [26] and Tweedy's chelation theory [27] might be used to explain the enhanced in antibacterial activity of the metal complexes.

Thus, using microwave assisted heating, two new zinc(II) and nickel(II) complexes with Schiff bases as ligands were obtained. Structures of the complexes have been confirmed by single crystal X-ray diffraction analysis. We found that microwave-assisted synthesis provides a clean, cheap and convenient method of heating that can result in the final products with less reaction time. The antibacterial property of the complexes was evaluated, which suggested that, in general, the metal complexes show somewhat enhanced antibacterial activity against the bacteria strains in comparison to the free Schiff bases. The complexes have strong activity against *Bacillus subtilis*.

Table 5. MIC values, μM

Compounds	*Staphylococcus aureus*	*Bacillus subtilis*	*Escherichia coli*	*Pseudomonas aeruginosa*
HL^1	128	64	128	256
HL^2	128	64	256	256
I	64	8	64	32
II	32	16	64	64
Ciprofloxacin	16	8	16	16

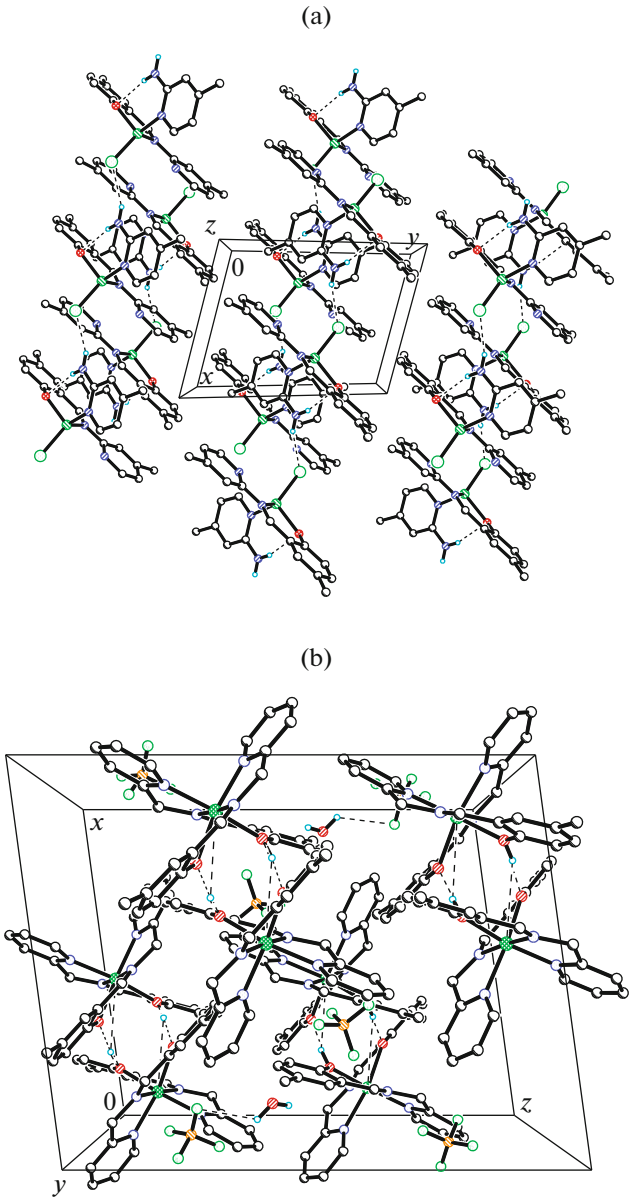

Fig. 2. Hydrogen bonds linked chain structure of complexes **I** (a) and **II** (b), viewed along the *z* axis for **I** and along the *x* axis for **II**. Hydrogen bonds are shown as dotted lines.

ACKNOWLEDGMENTS

Financial assistance from the Qiqihar University is gratefully acknowledged.

REFERENCES

1. Millos, C.J., Whittaker, A.G., and Brechin, E.K., *Polyhedron*, 2007, vol. 26, nos. 9–11, p. 1927.
2. Zhang, S.-H., Song, Y., Liang, H., et al., *CrystEngComm*, 2009, vol. 11, no. 5, p. 865.
3. Wang, X.-F., Zhang, Y.-B., Huang, H., et al., *Cryst. Growth Des.*, 2008, vol. 8, no. 12, p. 4559.
4. Zhang, S.-H., Zhou, Y.-L., Sun, X.-J., et al., *J. Solid State Chem.*, 2009, vol. 182, no. 11, p. 2991.
5. Zhang, S.-H. and Feng, C., *J. Mol. Struct.*, 2010, vol. 977, nos. 1–3, p. 62.
6. Saadeh, H.A., Abu Shaireh, E.A., Mosleh, I.M., et al., *Med. Chem. Res.*, 2012, vol. 21, no. 10, p. 2969.
7. Azizian, J., Mohammadi, M.K., Firuzi, O., et al., *Med. Chem. Res.*, 2012, vol. 21, no. 11, p. 3730.
8. Raza, R., Saeed, A., Arif, M., et al., *Chem. Biol. Drug Des.*, 2012, vol. 80, no. 4, p. 605.
9. Ghosh, M., Fleck, M., Mahanti, B., et al., *J. Coord. Chem.*, 2012, vol. 65, no. 22, p. 3884.
10. Mukherjee, P., Kar, P., Ianelli, S., et al., *Inorg. Chim. Acta*, 2011, vol. 365, no. 1, p. 318.
11. Bagherzadeh, M. and Amini, M., *Inorg. Chem. Commun.*, 2009, vol. 12, no. 1, p. 21.
12. Saghatforoush, L.A., Aminkhani, A., and Chalabian, F., *Transition Met. Chem.*, 2009, vol. 34, no. 8, p. 899.
13. Mohamed, E.M., Muralidharan, S., Panchanatheswaran, K., et al., *Acta Crystallogr., Sect C: Crystal Struct. Commun.*, 2003, vol. 59, no. 7, p. o367.
14. *SAINT, Area Detector Control and Integration Software*, Madison: Siemens Analytical X-ray Instruments Inc., 1996.
15. Sheldrick, G.M., *SHELXL-97 and SHELXTL Software Reference Manual*, Version 5.1, Madison: Brucker AXS Inc., 1997.
16. Sheldrick, G.M., *SADABS*, Göttingen: Univ. of Göttingen, 1996.
17. Burnett, M.N. and Jonnson, C.K., *ORTEP III, Report ORNL-6895*, Tennessee: Oak Ridge National Laboratory, 1996.
18. Singh, K., Kumar, Y., Puri, P., et al., *Med. Chem. Res.*, 2012, vol. 21, no. 8, p. 1708.
19. Okeke, M.I., Iroegbu, C.U., Eze, E.N., et al., *J. Ethnopharmacol.*, 2001, vol. 78, nos. 2–3, p. 119.
20. Sato, Y., Miyasaka, H., Matsumoto, N., et al., *Inorg. Chim. Acta*, 1996, vol. 247, no. 1, p. 57.
21. Guha, A., Chattopadhyay, T., Paul, N.D., et al., *Inorg. Chem.*, 2012, vol. 51, no. 16, p. 8750.
22. Chattopadhyay, T., Mukherjee, M., Banu, K.S., et al., *J. Coord. Chem.*, 2009, vol. 62, no. 6, p. 967.
23. Rotthaus, O., Labet, V., Philouze, C., et al., *Eur. J. Inorg. Chem.*, 2008, no. 27, p. 4215.
24. Jena, H.S., Subramanian, J., and Manivannan, V., *Inorg. Chim. Acta*, 2011, vol. 365, no. 1, p. 177.
25. Singh, K., Kumar, Y., Puri, P., et al., *Eur. J. Med. Chem.*, 2012, vol. 52, p. 313.
26. Raman, N., Kulandaisamy, A., and Jayasubramanian, K., *Polish J. Chem.*, 2002, vol. 76, no. 8, p. 1085.
27. Tweedy, B.G., *Phytopathology*, 1964, vol. 55, no. 5, p. 910.